PHYSICAL REVIEW A VOLUME 13, NUMBER 1 JANUARY 1976

# Incoherent x-ray scattering factors calculated from impulse-approximation Compton profiles: A comparison with the Waller-Hartree theory*

Hollace L. Cox, Jr.

*The University of Texas System Cancer Center, M. D. Anderson Hospital and Tumor Institute, Department of Pathology, Texas Medical Center, Houston, Texas 77025*

(Received 24 March 1975)

Incoherent x-ray scattering factors have been calculated for Li through Ne by integrating over Compton profiles calculated using the impulse approximation. Analytic expressions for the impulse-approximation Compton profiles (IACP) were derived from Clementi-Hartree-Fock (HF) analytic wave functions. Both experimental and theoretical HF electron binding energies were used in the numerical computation of the IACP inelastic scattering factors. These IACP scattering factors are compared with results obtained from the Waller-Hartree (WH) theory using HF atomic wave functions and a configuration-interaction (CI) wave function. Differences of as much as a factor of 2 are found at low scattering angles between the IACP and WH results calculated from HF wave functions. At low scattering angles the IACP results are in closer agreement with WH scattering factors calculated from the CI wave function than those computed from HF functions. A realistic possibility for obtaining more accurate inelastic scattering factors is demonstrated by direct integration over Compton profiles than can be computed from the WH scheme.

## I. INTRODUCTION

This paper reports the results of an investigation to compare x-ray inelastic scattering factors computed by direct integration of theoretical Compton profiles with those calculated using the Waller-Hartree (WH) theory.[1] The WH theory was considered to be the most successful of the early quantum-mechanical models to describe the inelastic scattering of x rays from a free atom and was superior to the theoretical models proposed by other authors.[2-5]

Because of the computational difficulties in applying the WH theory, a statistical treatment of this theory based upon the Thomas-Fermi (TF) model of the atom[6,7] was proposed by Heisenberg[8]; numerical values, calculated using Heisenberg's method, were tabulated by Bewilogua.[9] The tabulated Bewilogua factors were widely used by experimentalists to interpret x-ray and electron scattering data. Inelastic scattering factors could easily be obtained by interpolation for any atom over a wide range of incident photon energies and scattering angles. However, the Heisenberg-Bewilogua scattering factors did not agree as well with experimental results as did the WH factors, even when compared with early WH calculations based upon elementary wave functions. With the development of modern computers, many authors have calculated WH x-ray inelastic scattering factors using a wide variety of wave functions.[10-19]

The WH theory is now widely used to compute total inelastic scattering factors for x rays, but substantial differences have been reported between WH factors and incoherent scattering factors obtained directly from Compton profiles. Currat, DeCicco, and Weiss[20] found poor agreement at low scattering angles between WH scattering factors and total Compton cross sections calculated by integrating over theoretical Compton profiles. The Compton profiles they used had been computed by Weiss, Harvey and Phillips[21] using an impulse-approximation (IA) treatment of Compton scattering for the free-atom case. Currat *et al.* experimentally measured Compton profiles for Mo $K\alpha$ radiation scattered by Li, C, and Al, and found that the contribution to the profile due to the core electrons agreed with the free-atom IA profile calculations.[20] Total Compton cross sections, obtained by integrating the IA Compton profiles, were reported by them for Li and Ge and found to differ from WH inelastic scattering factors by as much as a factor of 3 at low scattering angles. These differences remained even after the application of the Bonham corrections[22] to the WH factors. Bonham[22] derived corrections to compensate for the errors introduced by the original assumptions which made it possible for the closure relationship to be used in deriving the final result for the WH expression.

The possibility of calculating more accurate inelastic x-ray scattering factors by direct integration over theoretical Compton profiles has been demonstrated by Mendelsohn and Biggs[23] and by B. J. Bloch and Mendelsohn.[24] These authors[23,24] used the exact, nonrelativistic formalism developed in 1934 by F. Bloch[25] to derive closed-form, analytic expressions for Compton profiles, and then integrated them to compute inelastic scattering factors. These scattering factors and profiles were restricted to hydrogen-atom wave functions, since hydrogen is the only case for which the (F.)

Bloch integrals can be solved in closed form.

To compare their results obtained from the "exact Bloch theory," these authors calculated hydrogenic scattering factors and Compton profiles using an application of the IA to the Bloch theory, a procedure rederived from first principles by Eisenberger and Platzman.[26] In both of these studies the hydrogenic Compton profiles calculated from the IA agreed closely with those obtained from the exact theory for cases of weak binding and high incident-photon energies.[23,24] Even when these conditions were not satisfied, there was sufficient crossing between the IA and exact profiles, in the region of the profile maximum, that values for the integrated IA and exact profiles differed by only a few percent. Therefore, both the "exact" and IA hydrogenic inelastic scattering factors were in close agreement over a wide range of incident photon energies, scattering angles, and electron binding energies. At low scattering angles and low momentum transfer, both the exact and IA scattering factors calculated by Bloch and Mendelsohn were substantially lower than the WH results and could differ from them by as much as 50%.[24]

Mendelsohn and Biggs[23] studied scattering from $K$ electrons and found that for Mo $K\alpha$ radiation scattered through 170° by atoms with effective $K$-shell nuclear charges up to $Z=20$, the maximum error for IA incoherent scattering factors was 15%.[23] WH factors calculated by them for the same scattering case differed from the exact results by 33% for $Z=10$ and by 400% for $Z=20$. These authors also demonstrated that total $K$-shell Compton cross sections cannot be described by an incoherent scattering factor which is a function of $(1/\lambda)\sin\theta$ only, as dictated by the WH theory.[23] Because the IA scattering factors agree closely with the exact values, Bloch and Mendelsohn concluded that more accurate incoherent scattering factors could be calculated for complex atoms by direct integration over IA Compton profiles than could be obtained using the WH scheme.[24]

In this research the calculation of inelastic scattering factors was extended to complex atoms using the IA and analytic Hartree-Fock (HF) wave functions compiled by Clementi.[27] Closed-form, analytic expressions for the impulse-approximation Compton profiles (IACP) were derived from the Clementi functions. The analytic IACP expressions were then numerically integrated to compute incoherent x-ray scattering factors. In 1968, Weiss, Harvey, and Phillips[21] extended the study of Compton profiles to complex atoms and derived analytic functions for Compton profiles from Clementi HF wave functions using the procedure described by Duncanson and Coulson.[28] Tabulated values of these profiles are listed in Ref. 21 for Li through Ge. Even though the Weiss tables are available, the independent derivation of analytic IACP expressions proved advantageous in computing the incoherent scattering factors obtained in this later study. These analytic functions provided a flexibility enabling the integration interval in $q$ and the range of $q$ to be varied as required for convergence to the final scattering-factor values.

The integrated IACP values computed in this study are compared with WH inelastic scattering factors[18,19] calculated from HF wave functions[27,29] and a configuration-interaction (CI) wave function.[30] This comparison supports the predictions made by Bloch and Mendelsohn.[24] Over a wide range of scattering angles, the IACP scattering factors are lower than all WH results calculated from HF wave functions and closely approach the WH values computed using the CI wave function. The shape and features of the IACP cross sections were compared and found to be in agreement with the IA hydrogenic profiles of Bloch and Mendelsohn[24] and the relativistic HF Compton profiles determined by Mendelsohn, Biggs, and Mann.[31]

The validity of the IA to represent the inelastic x-ray scattering case with sufficient accuracy to provide useful information is now well supported in the literature. Eisenberger and Platzman found that theoretical Compton profiles calculated from the IA were in extremely close agreement with experimentally measured profiles, with the exception of the portion attributed to deeply bound core electrons.[26] The theory provided by the IA relates the Compton profile directly to the ground-state electronic momentum distribution function. Experimental Compton-profile measurements have been studied to obtain information about atomic and molecular electronic momentum densities (EMD), and the Compton scattering from numerous gases[32-35] and solids[35-41] has been examined for this purpose. Solid-state Compton scattering measurements provide information concerning the EMD of conduction electrons; Phillips[38] has correlated the discontinuity in the experimental EMD profiles for polycrystalline Li, Be, Na, and Al with the Fermi momentum. EMD information is being obtained for heavier atoms from $\gamma$-ray Compton scattering.[42,43] The comparison between theoretical and experimental Compton profiles is now being considered as an additional test for the accuracy and validity of atomic and molecular wave functions.[44-46] In all of these cases the correlation between the experimental Compton profile and information related to the EMD has been made within the limits established by the IA model for the inelastic scattering of x rays. The possibility of using the Compton profile to compute inelastic scattering factors has long been ignored. Both the exact Bloch theory and the IA model describe the Compton scattering process more realistically than the WH theory. Scattering factors computed from either "exact" or IA Compton profiles should agree more accurately with experimental results than those calculated from the WH procedure.

## II. INCOHERENT SCATTERING FACTORS AND THE IACP

### A. Theory

This method used to calculate the IACP inelastic scattering factors is based upon a rigorous theory of Compton scattering that was first described by F. Bloch[25] and developed to a greater extent in the works of Eisenberger and Platzman,[26] Mendelsohn and Biggs,[23] and B. J. Bloch and Mendelsohn.[24] Using the following approach, F. Bloch obtained an expression for the Compton scattering cross section by retaining only the $A^2$ terms in the perturbation treatment of the nonrelativistic Schrödinger equation and applying the first Born approximation. The (F.) Bloch result is presented by Bloch and Mendelsohn as Eq. (6).[24] Eisenberger and Platzman[26] used this formalism to derive exact results for 1$S$ electrons, while Bloch and Mendelsohn extended this study to include $L$-shell electrons. The latter solved (F.) Bloch's equation by (i) choosing nonrelativistic bound state and continuum hydrogenic wave functions; (ii) transforming these functions to parabolic coordinates, a procedure followed earlier by Bloch[25]; and (iii) evaluating the integrals using residue calculus to obtain closed-form, analytic solutions. The $K$-shell[26] and $L$-shell[24] results determined by this theoretical procedure have been designated the "exact hydrogenic" results.

Although the exact Bloch[25] results represent a rigorous statement of the Compton scattering process, analytic solutions can only be obtained for hydrogenic wave functions. Numerical solutions of Bloch's equation are possible for complex atoms, but the application of the IA to the Bloch theory enables Compton profiles to be easily calculated for complicated atomic and molecular wave functions. Eisenberger and Platzman derived the IA results from first principles by taking the Fourier integral representation of the δ function and applying time-dependent perturbation theory.[26] These authors demonstrated that when the energy transfer is large enough the interaction time is extremely short and the atomic potential field acting on the electron is constant. The form for the IACP result used in this research is the same as Eq. (10) in the Bloch and Mendelsohn paper.[24]

In Eq. (10) of Ref. 24, $J_{\text{imp}}(q)$ is the Compton profile as first derived by DuMond using the IA.[47,48] This function is expressed in the following equation for a system of electrons with an isotropic momentum distribution:

$$J_{\text{imp}}(q) = 2\pi \int_{|q|}^{\infty} |\chi(p_1)|^2 p_1 \, dp_1 \, . \tag{1}$$

The quantity $\chi(p_1)$ is the momentum representation of the atomic wave function. The parameter $q$ is described by DuMond as the projection of $p_1$, the individual electron momentum before collision, upon a unit vector in the direction of the momentum transfer ($\vec{K}$).[47,48] Equation (2) defines $q$ as

$$q = \vec{p}_1 \cdot \vec{K} / |\vec{K}| \, . \tag{2}$$

The momentum transfer $\vec{K}$ is defined as $\vec{K} = \vec{k}_1 - \vec{k}_2$, where $\vec{k}_1$ and $\vec{k}_2$ represent the incident and scattered photon wave vectors, respectively.

Total free-atom incoherent scattering factors are easily calculated by integrating Eq. (10) of Ref. 24, over the energy transferred in the photon-electron collision. This technique was suggested by Bloch and Mendelsohn.[24] Equation (3) used in this program to compute the IACP incoherent scattering factors is identical to Eq. (19) in Ref. 24:

$$S(E_1, 2\theta) = \frac{1}{27.212} \int_{|e_0|}^{E_1} \frac{1}{\kappa} \left( \frac{E_2}{E_1} \right) J_{\text{imp}}(q) \, dE \, . \tag{3}$$

The energy transferred in the collision process is given by $E = E_1 - E_2$, where $E_1$ and $E_2$ are the incident and scattered photon energies. The parameter $\kappa$ is proportional to $K$ and given by $\kappa^2 = K^2 a_0^2$, where $a_0$ is the nonrelativistic first Bohr radius for the hydrogen atom. The integration limits are taken between the electron binding energy, $|e_0|$, and the energy of the incident x-ray photon, $E_1$. In the work reported here, the integration variable was transformed to $dq$ and the integration was carried out over the appropriate limits in $q$, a procedure to be described in more detail later in the text.

### B. Method of Calculation

Incoherent scattering factors were obtained by a straightforward procedure using Eqs. (1) and (3). Clementi HF wave functions[27] were chosen as the atomic wave functions for this calculation because they are compact, closed-form, analytic expressions, and accurate enough to obey the virial theorem to eight significant figures. Another reason for the choice of Clementi functions is that WH incoherent scattering factors calculated from these functions are available in the literature for comparison.[18,19]

The position-space Clementi orbital functions[27] are given by the following general form:

$$\Psi_{nl}(r) = \sum_i C_i N_i r^{n_i - 1} e^{-\alpha_i r} Y_{lm}(\theta, \varphi) . \tag{4}$$

Momentum-space representations of the Clementi wave functions were derived using the standard Fourier-transformation procedure defined in Eq. (5) as

$$\chi(p) = \frac{1}{(2\pi)^{3/2}} \int_{\vec{r}} e^{i\vec{k}\cdot\vec{r}} \psi(\vec{r})\, d\vec{r} . \tag{5}$$

Since the Clementi 1$S$ and 2$S$ orbital functions have the same functional form and differ only in their expansion coefficients, the momentum-space representation for the $S$ orbital functions is

$$\chi_{ns}(p) = \frac{\sqrt{2}}{\pi} \left( \sum_{i=1}^{2} \frac{C_i(ns) N_i \alpha_i}{(p^2 + \alpha_i^2)^2} + \sum_{j=3}^{6} \frac{C_j(ns) N_j (3\alpha_j - p^2)}{(\alpha_j^2 + p^2)^3} \right), \tag{6}$$

with $n = 1, 2$.

The $m$ subspace is not defined for the Clementi orbital functions. Therefore, only one form remains after Fourier transformation for the momentum-space representation of the $P$ orbitals, and it is given by

$$\chi_{2P}(p) = \left( \frac{96}{\pi 2} \right)^{1/2} (i) \sum_{i=1}^{4} \frac{C_i(2p) N_i \alpha_i p}{(\alpha_i^2 + p^2)^3} . \tag{7}$$

The $C_i$'s and $N_i$'s in Eqs. (4), (6), and (7) are expansion coefficients and normalization factors, respectively, while the $\alpha_i$'s are pre-exponential factors. All are from the original Clementi wave functions. Equations (4), (6), and (7) are expressed in atomic units.

The results from Eqs. (6) and (7) were then used to derive closed-form analytic expressions for the Compton profile, $J(q)$, defined in Eq. (1). All integrals were solved using standard integration procedures and a technique derived from the residue theorem, described briefly in the Appendix. Although analytic expressions for $J(q)$ were derived by Weiss, Harvey, and Phillips, only their numerical results were published.[21] The analytic functions for $J(q)$ derived in this research were not only useful for the incoherent scattering-factor calculations but were required for the computation of scattering factors evaluated at small scattering angles. They provided an over-all flexibility for the range of $q$ and incremental $q$ intervals chosen for the numerical integration of Eq. (3). Because of their contribution to the accuracy of the final scattering-factor results, the general forms for these expressions are given in Eqs. (8)–(16).

The expression obtained for $J_{ns}(q)$ is given as

$$J_{ns}(q) = \frac{4}{\pi} \sum_{i=1}^{2} \beta_i^2 I(1) + \frac{8}{\pi} \sum_{i<j}^{2} \sum^{2} \beta_i \beta_j I(2) + \frac{4}{\pi} \sum_{j=3}^{6} \gamma_j^2 I(3) + \frac{8}{\pi} \sum_{i=3}^{5} \sum_{<k}^{6} \gamma_i \gamma_k I(4) + \frac{8}{\pi} \sum_{i=1}^{2} \sum_{j=3}^{6} \beta_i \gamma_j I(5) , \tag{8}$$

where

$$I(1) = \frac{1}{6(q^2 + \alpha_i^2)^3} , \tag{9}$$

$$I(2) = \frac{1}{2(\alpha_j^2 - \alpha_i^2)^2} \left( \frac{2q^2 + \alpha_i^2 + \alpha_j^2}{(q^2 + \alpha_i^2)(q^2 + \alpha_j^2)} \right) + \frac{1}{(\alpha_j^2 - \alpha_i^2)^3} \ln\left( \frac{q^2 + \alpha_j^2}{q^2 + \alpha_i^2} \right), \tag{10}$$

$$I(3) = \frac{5(q^2 - 2\alpha_j^2)^2 + 3\alpha_j^4}{30(q^2 + \alpha_j^2)^5} , \tag{11}$$

$$\begin{aligned} I(4) = {} & \frac{-3}{4(\alpha_k^2 - \alpha_j^2)^4} \left( \frac{(25\alpha_k^2 + 7\alpha_j^2)\alpha_j^2}{q^2 + \alpha_j^2} + \frac{(25\alpha_j^2 + 7\alpha_k^2)\alpha_k^2}{q^2 + \alpha_k^2} \right) \\ & + \frac{1}{4(\alpha_k^2 - \alpha_j^2)^3} \left( \frac{6\alpha_k^2(\alpha_j^2 - q^2) - \alpha_j^2(7q^2 + 3\alpha_j^2)}{(q^2 + \alpha_j^2)^2} - \frac{[6\alpha_j^2(\alpha_k^2 - q^2) - (7q^2 + \alpha_k^2)\alpha_k^2]}{(q^2 + \alpha_k^2)^2} \right) \\ & + \frac{5(\alpha_k^2 + \alpha_j^2)^2 + 28\alpha_j^2\alpha_k^2}{(\alpha_k^2 - \alpha_j^2)^5} \ln\left( \frac{q^2 + \alpha_k^2}{q^2 + \alpha_j^2} \right), \end{aligned} \tag{12}$$

and

$$I(5) = \frac{1}{2(\alpha_j^2 - \alpha_i^2)^3} \left( \frac{7\alpha_j^2 + \alpha_i^2}{q^2 + \alpha_j^2} + \frac{3\alpha_j^2 + \alpha_i^2}{q^2 + \alpha_i^2} \right) + \frac{\alpha_j^2}{(\alpha_j^2 - \alpha_i^2)^2 (q^2 + \alpha_j^2)^2} - \frac{(5\alpha_j^2 + \alpha_i^2)}{(\alpha_j^2 - \alpha_i^2)^4} \ln\left( \frac{q^2 + \alpha_j^2}{q^2 + \alpha_i^2} \right) . \tag{13}$$

Similar results were obtained for the $P$ orbitals, and $J_{2p}$ is given as

$$J_{2p}(q)=\frac{64}{\pi}\left(\sum_{i=1}^{4}\epsilon_i^2 I_p(1)+2\sum_{i>j=1}^{4}\sum^{4}\epsilon_i\epsilon_j I_p(2)\right), \tag{14}$$

where

$$I_p(1)=\frac{5q^2+\alpha_i^2}{40(q^2+\alpha_i^2)^5}, \tag{15}$$

and

$$I_p(2)=\frac{3}{2(\alpha_j^2-\alpha_i^2)^4}\left(\frac{\alpha_i^2}{q^2+\alpha_i^2}+\frac{\alpha_j^2}{q^2+\alpha_j^2}\right)+\frac{1}{4(\alpha_j^2-\alpha_i^2)^3}\left(\frac{2q^2+\alpha_i^2}{(q^2+\alpha_i^2)^2}-\frac{2q^2+\alpha_j^2}{(q^2+\alpha_j^2)^2}\right)-\frac{3(\alpha_j^2+\alpha_i^2)}{2(\alpha_j^2-\alpha_i^2)^5}\ln\left(\frac{q^2+\alpha_j^2}{q^2+\alpha_i^2}\right). \tag{16}$$

In Eqs. (8) and (14) the coefficients $\beta_i$, $\gamma_i$, and $\epsilon_i$ are constants containing appropriate combinations of expansion coefficients and normalization constants from the original position-space HF wave functions.

A relationship for the energy ratio $E_2/E_1$ was obtained from the DuMond expression[47,48] for the wavelength dispersion about the Compton-scattered peak and used in calculating scattering factors from Eq. (3). The change in the scattered wavelength $\lambda_2$, derived by DuMond[47,48] and Cooper[49] from nonrelativistic energy and momentum conservation equations, is expressed in Eq. (17) as

$$\lambda_2-\lambda_1=\frac{2h}{m_0c}\sin^2\theta-\left(\frac{2(\lambda_1\lambda_2)^{1/2}}{m_0c}\sin\theta\right)q, \tag{17}$$

where $\lambda_1$ and $\lambda_2$ are the incident and scattered photon wavelengths, respectively. After some algebraic manipulation the $E_2/E_1$ ratio is easily derived from Eq. (17) and defined as $\epsilon$, given by

$$\epsilon\equiv\frac{E_2}{E_1}=\frac{2}{2\alpha+\beta^2q^2+\beta q(4\alpha+\beta^2q^2)^{1/2}}, \tag{18}$$

where

$$\alpha=1+(2E_1/m_0c^2)\sin^2\theta \tag{19}$$

and

$$\beta=(2\sin\theta)/m_0c. \tag{20}$$

At $q=0$, Eq. (18) reduces to the well-known energy shift between the Compton and the elastically scattered peak centers.[50] For convenience, $\kappa$ was reexpressed in terms of the incident photon energy, energy transfer, and scattering angle, as

$$\kappa=C_0[4E_1(E_1-E)\sin^2\theta+E^2], \tag{21}$$

with

$$C_0=(\hbar/me^2c)^2. \tag{22}$$

The integration variable $dE$ in Eq. (3) was transformed to allow the integration to be performed over $q$:

$$dE=E_1|d\epsilon/dq|\,dq. \tag{23}$$

By using Eq. (18) and the energy-transfer relationship, the lower integration limit was derived in terms of $q$ and defined as $q^m_{(nl)}$ by

$$q^m_{(nl)}=\left[\frac{m_0c}{2\sin\theta}\left(\frac{1}{\epsilon_m}-1\right)-\frac{E_1}{C}\sin\theta\right]\epsilon_m^{1/2}, \tag{24}$$

where

$$\epsilon_m=1-|e_0(nl)|/E_1. \tag{25}$$

In Eq. (25), $|e_0(nl)|$ is the binding energy for each $nl$ electron. The lower integration limit is established by $q^m(nl)$, and it is obvious from Eqs. (18) and (24) that when the energy transfer ($E$) equals $E_1$, the upper integration limit in $q$ must be infinite.

### C. Numerical procedures

The numerical integration of Eq. (3) was carried out using Simpson's rule.[51] In order to be consistent with the Clementi functions, $q^m$ and $q$ were computed in atomic units, and the $q$ integration was taken over a range between $q^m$ and $q=40$. Numerical convergence for the scattering factors themselves was assured by choosing increments in $q$ ($\Delta q$) of 0.1, 0.05 and 0.025, involving 400, 800, and 1600 Simpson's-rule intervals, respec-

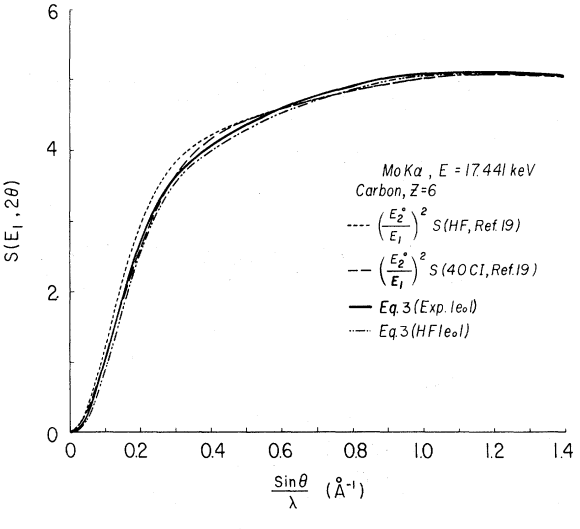

FIG. 1. Comparison between WH incoherent scattering factors computed by Brown (Ref. 19) and IACP scattering factors calculated from Eq. (3).

tively, and the upper-$q$ limit was extended to $q = 60$ in some cases. A Simpson's-rule integration was performed within the $q$ interval containing $q^m$, to ensure that $q^m$ was the absolute starting point. Convergence to six significant figures was required in the integration of Eq. (3), and there was no evidence of numerical instability in the IACP's over the ranges in $q$ used in the integration. For scattering angles larger than 40°, this convergence criterion was satisfied for $\Delta q = 0.1$, and $\Delta q = 0.025$ was needed only for scattering angles less than 1.0°. The numerical accuracy of the IACP's and the scattering factors calculated from them are limited only by the input HF wave-function parameters given in the Clementi table.[27]

The x-ray wavelengths and energies used in these calculations were obtained from tables prepared by Bearden[52] and from the ASTM tables.[53] All calculations in a.u. were carried out with 1 Hartree = 27.212 eV, and using a value for the fine-structure constant of $\alpha^{-1} = 137.036\,08$, reported by Adler.[54] Experimental electron binding energies (Exp. $E_B$) were chosen from the free-atom values compiled by Lotz.[55] To determine the effects different binding energies have upon scattering factors, Clementi HF orbital energies[27] were used to approximate theoretical free-atom binding energies; these energies have been designated HF $E_B$.

## III. RESULTS AND DISCUSSION

IACP curves were calculated in terms of $(d\sigma/dE\, d\Omega)_{\text{imp}}/(d\sigma/d\Omega)_T$ using Eq. (10) of Ref. 24 for scattering from Li through Ne and covering a wide range of incident photon energies and scat-

TABLE I. Comparison of Waller-Hartree and IACP incoherent scattering factors; Mo $K\alpha$ radiation scattered by carbon, $Z=6$. $E_1 = 17.441$ keV, $\lambda = 0.710\,73$ Å.

| $\frac{\sin\theta}{\lambda}$ (Å$^{-1}$) | $\left(\frac{E_2^0}{E_1}\right)^2 S(\text{HF})$ [a] | $\left(\frac{E_2^0}{E_1}\right)^2 S(\text{CI})$ [b] | $S(\text{CPHF})$ [c] | $S(\text{CPEX})$ [d] | $S(\text{CPEX})$ [e] |
|---|---|---|---|---|---|
| 0.005 | 0.004 472 | 0.003 791 | 0.000 02 | 0.000 04 | 0.000 04 |
| 0.006 | 0.005 932 | 0.004 953 | 0.000 06 | 0.000 11 | 0.000 11 |
| 0.008 | 0.009 666 | 0.007 929 | 0.000 23 | 0.000 41 | 0.000 41 |
| 0.010 | 0.015 70 | 0.012 99 | 0.000 65 | 0.001 10 | 0.001 10 |
| 0.020 | 0.060 00 | 0.051 64 | 0.012 26 | 0.017 11 | 0.017 11 |
| 0.030 | 0.1337 | 0.1157 | 0.051 26 | 0.063 20 | 0.063 20 |
| 0.040 | 0.2326 | 0.2015 | 0.120 05 | 0.138 40 | 0.138 40 |
| 0.050 | 0.3558 | 0.3085 | 0.212 61 | 0.237 95 | 0.237 96 |
| 0.060 | 0.4992 | 0.4316 | 0.322 56 | 0.358 05 | 0.358 07 |
| 0.080 | 0.8329 | 0.7195 | 0.579 32 | 0.648 70 | 0.648 79 |
| 0.10 | 1.2043 | 1.0385 | 0.876 35 | 0.989 02 | 0.989 26 |
| 0.15 | 2.1407 | 1.8633 | 1.737 86 | 1.902 54 | 1.903 89 |
| 0.20 | 2.9081 | 2.5969 | 2.548 83 | 2.673 74 | 2.677 61 |
| 0.25 | 3.4486 | 3.1842 | 3.137 67 | 3.212 19 | 3.219 99 |
| 0.30 | 3.8038 | 3.6201 | 3.525 86 | 3.570 71 | 3.583 24 |
| 0.35 | 4.0356 | 3.9264 | 3.788 32 | 3.820 37 | 3.837 64 |
| 0.40 | 4.1948 | 4.1379 | 3.982 09 | 4.010 00 | 4.031 32 |
| 0.45 | 4.3137 | 4.2878 | 4.139 36 | 4.166 67 | 4.190 96 |
| 0.50 | 4.4117 | 4.4015 | 4.276 05 | 4.303 66 | 4.329 73 |
| 0.60 | 4.5757 | 4.5760 | 4.510 95 | 4.538 31 | 4.564 77 |
| 0.70 | 4.7155 | 4.7171 | 4.703 45 | 4.728 35 | 4.572 34 |
| 0.8 | 4.8339 | 4.8353 | 4.853 56 | 4.874 71 | 4.894 96 |
| 0.9 | 4.9284 | 4.9293 | 4.961 88 | 4.979 05 | 4.995 41 |
| 1.0 | 4.9967 | 4.9979 | 5.031 74 | 5.045 28 | 5.058 14 |
| 1.1 | 5.0388 | 5.0395 | 5.067 92 | 5.078 42 | 5.088 38 |
| 1.2 | 5.0556 | 5.0562 | 5.075 57 | 5.083 62 | 5.091 27 |
| 1.3 | 5.0492 | 5.0498 | 5.059 48 | 5.065 63 | 5.071 47 |
| 1.4 | 5.0224 | 5.0228 | 5.023 85 | 5.028 54 | 5.033 00 |

[a] Waller-Hartree scattering factors calculated using a HF wave function (Ref. 19).

[b] Waller-Hartree scattering factors calculated using a 40 term CI wave function (Ref. 19).

[c] IACP scattering factors calculated from Eq. (3) using HF orbital energies for electron binding energies.

[d] IACP scattering factors calculated from Eq. (3): 1$S$ binding energy obtained from Ref. 60; 2$S$ and 2$P$ experimental binding energies from Ref. 55.

[e] IACP scattering factors calculated from Eq. (3) using experimental binding energies, Ref. 55.

TABLE II. Comparison between Waller-Hartree and IACP scattering factors; W $K\alpha$ radiation scattered by carbon, $Z=6$. $E_1=58.856$ keV, $\lambda=0.210\,62$ Å.

| $\frac{\sin\theta}{\lambda}$ (Å$^{-1}$) | $\left(\frac{E_2^0}{E_1}\right)^2$ $S$(HF)[a] | $\left(\frac{E_2^0}{E_1}\right)^2$ $S$(CI)[b] | $S$(CPHF)[c] | $S$(CPEX)[d] |
|---|---|---|---|---|
| 0.05 | 0.3559 | 0.3086 | 0.213 01 | 0.238 39 |
| 0.10 | 1.2048 | 1.0390 | 0.878 34 | 0.991 43 |
| 0.15 | 2.1430 | 1.8653 | 1.742 99 | 1.909 22 |
| 0.20 | 2.9147 | 2.6020 | 2.558 51 | 2.687 54 |
| 0.25 | 3.4591 | 3.1938 | 3.153 42 | 3.236 15 |
| 0.30 | 3.8204 | 3.6359 | 3.549 42 | 3.607 43 |
| 0.35 | 4.0596 | 3.9497 | 3.821 48 | 3.871 58 |
| 0.40 | 4.2274 | 4.1700 | 4.026 52 | 4.076 61 |
| 0.45 | 4.3561 | 4.3300 | 4.196 59 | 4.249 04 |
| 0.50 | 4.4653 | 4.4549 | 4.347 44 | 4.401 92 |
| 0.60 | 4.6557 | 4.6560 | 4.614 38 | 4.668 75 |
| 0.70 | 4.8277 | 4.8293 | 4.843 37 | 4.892 56 |
| 0.8 | 4.9838 | 4.9857 | 5.034 12 | 5.075 63 |
| 0.9 | 5.1224 | 5.1233 | 5.187 05 | 5.220 57 |
| 1.0 | 5.2396 | 5.2409 | 5.305 31 | 5.331 64 |
| 1.1 | 5.3353 | 5.3360 | 5.393 46 | 5.413 81 |
| 1.2 | 5.4097 | 5.4104 | 5.456 35 | 5.471 94 |
| 1.3 | 5.4645 | 5.4650 | 5.498 45 | 5.510 34 |
| 1.4 | 5.5015 | 5.5020 | 5.523 60 | 5.532 65 |
| 1.5 | 5.5233 | 5.5237 | 5.534 95 | 5.541 86 |
| 1.6 | 5.5320 | 5.5325 | 5.535 08 | 5.540 37 |
| 1.8 | 5.5182 | 5.5185 | 5.509 40 | 5.512 53 |
| 2.0 | 5.4736 | 5.4736 | 5.458 29 | 5.460 18 |
| 2.2 | 5.4073 | 5.4074 | 5.389 11 | 5.390 29 |
| 2.4 | 5.3259 | 5.3260 | 5.306 61 | 5.307 35 |
| 2.6 | 5.2333 | 5.2333 | 5.213 91 | 5.214 39 |
| 2.8 | 5.1323 | 5.1324 | 5.113 23 | 5.113 55 |
| 3.0 | 5.0250 | 5.0250 | 5.006 17 | 5.006 39 |
| 3.2 | 4.9126 | 4.9126 | 4.894 00 | 4.894 14 |
| 3.4 | 4.7962 | 4.7962 | 4.777 73 | 4.777 83 |
| 3.6 | 4.6767 | 4.6767 | 4.658 23 | 4.658 31 |
| 3.8 | 4.5549 | 4.5549 | 4.536 27 | 4.536 33 |
| 4.0 | 4.4313 | 4.4313 | 4.412 52 | 4.412 55 |

[a] Waller-Hartree scattering factors calculated using a HF wave function (Ref. 19).

[b] Waller-Hartree scattering factors calculated using a 40 term CI wave function (Ref. 19).

[c] IACP scattering factors calculated from Eq. (3) using HF orbital energies for electron binding energies.

[d] IACP scattering factors calculated from Eq. (3) using experimental binding energies, Ref. 55.

tering angles. These curves are not reported here since they contain the same features as the IA hydrogenic Compton profiles reported by Bloch and Mendelsohn.[24] A zero-slope region was found in the 2$S$ $J_{\text{imp}}(q)$ profiles, corresponding to a node in the 2$S$ momentum-space wave functions calculated from Eq. (6) for all atoms studied. This finding agreed with the 2$S$ IA Bloch and Mendelsohn profiles[24] and the 2$S$ relativistic HF Compton profiles obtained by Mendelsohn, Biggs, and Mann.[31] Bloch and Mendelsohn derived a $Z/2$ dependence for $q^0$ (the value of $q$ at the zero-slope position) for the $J_{\text{imp}}^{2S}(q)$ profile.[24] In this research a similar dependence on $Z$ was found for $q^0$. Using $\Delta q$ increments of 0.05 and 0.025, $q^0$ was established to be 1.5 for lithium, 1.85 and 2.25 for boron and carbon, respectively, and increased to 4.05 for neon.

Because of the $E_2/E_1$ dependence in the integrand of Eq. (3), the IACP factors have a specificity determined by the incident radiation. In order to compare the WH scattering factors with the IACP factors, the WH values were multiplied by $(E_2^0/E_1)^2$ over the $s$ and $q_T$ range used in these calculations. One of the approximations made in the derivation of the final WH scattering factor expression assumes that $(E_2/E_1)^2$ is 1, a condition which is not true for the strong-binding case. Currat *et al.* chose $(E_2^0/E_1)^2$ as a suitable average of $(E_2/E_1)^2$ and defined their WH expressions in terms of $(E_2^0/E_1)^2$ as a multiplicative factor.[20] For addition-

TABLE III. Comparison between Tavard's Waller-Hartree and the IACP results; Mo $K\alpha$ radiation scattered by B through Ne. $E_1=17.441$ keV, $\lambda=0.710\,73$ Å.

| $q_T$ (Å$^{-1}$) [a] | $\frac{\sin\theta}{\lambda}$ (Å$^{-1}$) | $\left(\frac{E_2^0}{E_1}\right)^2 S(\mathrm{THF})$ [b] | $S(\mathrm{CPHF})$ [c] | $S(\mathrm{CPEX})$ [d] | $\left(\frac{E_2^0}{E_1}\right)^2 S(\mathrm{THF})$ [b] | $S(\mathrm{CPHF})$ [c] | $S(\mathrm{CPEX})$ [d] |
|---|---|---|---|---|---|---|---|
| | | | B, $Z=5$ | | | C, $Z=6$ | |
| 0.4 | 0.031 83 | 0.188 | 0.053 52 | 0.056 61 | 0.150 | 0.061 76 | 0.074 94 |
| 0.8 | 0.063 66 | 0.674 | 0.268 29 | 0.279 93 | 0.556 | 0.366 24 | 0.406 62 |
| 1.2 | 0.095 49 | 1.287 | 0.669 55 | 0.704 92 | 1.116 | 0.806 10 | 0.909 35 |
| 1.4 | 0.111 41 | 1.590 | 0.938 59 | 0.983 56 | 1.420 | 1.061 89 | 1.196 86 |
| 1.8 | 0.143 24 | 2.122 | 1.516 48 | 1.566 33 | 2.013 | 1.617 81 | 1.783 55 |
| 2.2 | 0.175 07 | 2.527 | 2.022 20 | 2.066 71 | 2.543 | 2.167 38 | 2.320 44 |
| 2.6 | 0.206 90 | 2.812 | 2.399 81 | 2.440 09 | 2.982 | 2.644 39 | 2.765 75 |
| 3.6 | 0.286 48 | 3.195 | 2.933 81 | 2.981 71 | 3.709 | 3.436 27 | 2.498 39 |
| 4.0 | 0.318 31 | 3.285 | 3.065 09 | 3.119 21 | 3.887 | 3.632 95 | 3.685 92 |
| 6.0 | 0.477 46 | 3.624 | 3.558 39 | 3.627 02 | 4.364 | 4.216 40 | 4.269 28 |
| 8.0 | 0.636 62 | 3.912 | 3.933 28 | 3.988 22 | 4.628 | 4.586 30 | 4.638 77 |
| 9.2 | 0.732 11 | 4.053 | 4.094 62 | 4.137 91 | 4.756 | 4.756 30 | 4.802 94 |
| 10.0 | 0.795 77 | 4.131 | 4.175 71 | 4.211 78 | 4.829 | 4.848 07 | 4.889 82 |
| 11.0 | 0.875 35 | 4.209 | 4.250 20 | 4.278 48 | 4.907 | 4.938 92 | 4.974 35 |
| 12.0 | 0.954 93 | 4.266 | 4.298 66 | 4.320 60 | 4.970 | 5.004 72 | 5.034 21 |
| 13.0 | 1.034 51 | 4.302 | 4.325 18 | 4.342 10 | 5.014 | 5.047 76 | 5.071 98 |
| 14.0 | 1.114 08 | 4.319 | 4.333 48 | 4.346 49 | 5.043 | 5.070 60 | 5.090 32 |
| 15.0 | 1.193 66 | 4.320 | 4.326 74 | 4.336 76 | 5.055 | 5.075 83 | 5.091 80 |
| 16.0 | 1.273 24 | 4.309 | 4.307 63 | 4.315 35 | 5.053 | 5.065 86 | 5.078 75 |
| 17.0 | 1.352 82 | 4.285 | 4.278 33 | 4.284 31 | 5.037 | 5.042 85 | 5.053 25 |
| | | | N, $Z=7$ | | | O, $Z=8$ | |
| 0.4 | 0.031 83 | 0.123 | 0.063 43 | 0.084 78 | 0.111 | 0.085 29 | 0.171 43 |
| 0.8 | 0.063 66 | 0.467 | 0.429 28 | 0.492 14 | 0.426 | 0.565 92 | 0.821 56 |
| 1.2 | 0.095 49 | 0.965 | 0.933 58 | 1.076 25 | 0.892 | 1.158 47 | 1.455 85 |
| 1.4 | 0.111 41 | 1.247 | 1.200 39 | 1.388 35 | 1.164 | 1.442 83 | 1.746 20 |
| 1.8 | 0.143 24 | 1.831 | 1.751 59 | 2.001 23 | 1.746 | 1.992 25 | 2.307 27 |
| 2.2 | 0.175 07 | 2.399 | 2.305 94 | 2.562 09 | 2.338 | 2.533 34 | 2.849 02 |
| 2.6 | 0.206 90 | 2.914 | 2.824 70 | 3.048 83 | 2.904 | 3.058 92 | 3.353 42 |
| 3.6 | 0.286 48 | 3.914 | 3.815 09 | 3.932 66 | 4.103 | 4.166 82 | 4.358 22 |
| 4.0 | 0.318 31 | 4.203 | 4.088 26 | 4.177 13 | 4.481 | 4.502 27 | 4.655 05 |
| 6.0 | 0.477 46 | 5.019 | 4.865 48 | 4.909 78 | 5.643 | 5.493 73 | 5.551 89 |
| 8.0 | 0.636 62 | 5.358 | 5.262 48 | 5.306 74 | 6.102 | 5.948 01 | 5.990 30 |
| 9.2 | 0.732 11 | 5.486 | 5.434 93 | 5.477 69 | 6.244 | 6.126 40 | 6.166 29 |
| 10.0 | 0.795 77 | 5.556 | 5.529 66 | 5.570 19 | 6.311 | 6.222 15 | 6.260 52 |
| 11.0 | 0.875 35 | 5.628 | 5.626 60 | 5.663 41 | 6.378 | 6.320 20 | 6.356 25 |
| 12.0 | 0.954 93 | 5.686 | 5.700 59 | 5.733 18 | 6.427 | 6.396 31 | 6.429 55 |
| 13.0 | 1.034 51 | 5.729 | 5.752 82 | 5.781 13 | 6.463 | 6.451 84 | 6.481 94 |
| 14.0 | 1.114 08 | 5.759 | 5.784 90 | 5.809 14 | 6.486 | 6.487 99 | 6.514 83 |
| 15.0 | 1.193 66 | 5.775 | 5.798 60 | 5.819 16 | 6.497 | 6.505 97 | 6.529 62 |
| 16.0 | 1.273 24 | 5.775 | 5.795 79 | 5.813 11 | 6.496 | 6.507 15 | 6.527 80 |
| 17.0 | 1.352 82 | 5.764 | 5.778 32 | 5.792 83 | 6.482 | 6.493 00 | 6.510 89 |
| | | | F, $Z=9$ | | | Ne, $Z=10$ | |
| 0.4 | 0.031 83 | 0.100 | 0.097 36 | 0.148 62 | 0.09 | 0.101 27 | 0.129 09 |
| 0.8 | 0.063 66 | 0.385 | 0.656 63 | 0.824 12 | 0.35 | 0.712 26 | 0.813 00 |
| 1.2 | 0.095 49 | 0.817 | 1.334 93 | 1.535 27 | 0.75 | 1.468 58 | 1.594 18 |
| 1.4 | 0.111 41 | 1.073 | 1.648 42 | 1.851 62 | 0.99 | 1.816 01 | 1.943 48 |
| 1.8 | 0.143 24 | 1.634 | 2.224 22 | 2.433 67 | 1.52 | 2.436 12 | 2.565 56 |
| 2.2 | 0.175 07 | 2.221 | 2.765 17 | 2.981 93 | 2.09 | 2.992 76 | 3.127 39 |
| 2.6 | 0.206 90 | 2.805 | 3.289 46 | 3.504 47 | 2.66 | 3.519 72 | 3.658 09 |
| 3.6 | 0.286 48 | 4.120 | 4.463 06 | 4.626 90 | 4.03 | 4.728 67 | 4.849 27 |
| 4.0 | 0.318 31 | 4.565 | 4.846 91 | 4.983 97 | 4.52 | 5.146 66 | 5.252 51 |
| 6.0 | 0.477 46 | 6.086 | 6.064 34 | 6.117 39 | 6.35 | 6.573 65 | 6.618 53 |
| 8.0 | 0.636 62 | 6.769 | 6.617 68 | 6.651 05 | 7.30 | 7.254 33 | 7.279 69 |
| 9.2 | 0.732 11 | 6.968 | 6.816 41 | 6.847 30 | 7.61 | 7.488 89 | 7.511 39 |

TABLE III *(Continued)*

| $q_T$ (Å$^{-1}$) [a] | $\frac{\sin\theta}{\lambda}$ (Å$^{-1}$) | $\left(\frac{E_2^0}{E_1}\right)^2$ $S$(THF) [b] | $S$(CPHF) [c] | $S$(CPEX) [d] | $\left(\frac{E_2^0}{E_1}\right)^2$ $S$(THF) [b] | $S$(CPHF) [c] | $S$(CPEX) [d] |
|---|---|---|---|---|---|---|---|
| 10.0 | 0.795 77 | 7.054 | 6.918 00 | 6.948 15 | 7.73 | 7.603 92 | 7.625 69 |
| 11.0 | 0.875 35 | 7.128 | 7.019 22 | 7.048 40 | 7.84 | 7.714 36 | 7.735 72 |
| 12.0 | 0.954 93 | 7.178 | 7.096 42 | 7.124 35 | 7.90 | 7.795 79 | 7.816 71 |
| 13.0 | 1.034 51 | 7.209 | 7.152 53 | 7.178 84 | 7.94 | 7.853 26 | 7.873 58 |
| 14.0 | 1.114 08 | 7.225 | 7.189 36 | 7.213 74 | 7.96 | 7.890 05 | 7.909 51 |
| 15.0 | 1.193 66 | 7.229 | 7.208 19 | 7.230 50 | 7.97 | 7.908 18 | 7.926 55 |
| 16.0 | 1.273 24 | 7.221 | 7.210 26 | 7.230 40 | 7.95 | 7.909 17 | 7.926 30 |
| 17.0 | 1.352 82 | 7.201 | 7.196 76 | 7.214 78 | 7.93 | 7.894 36 | 7.910 15 |

[a] $q_T = (4\pi \sin\theta)/\lambda$.

[b] Tavard's incoherent scattering factors, Ref. 18; calculated from Clementi HF wave functions, Ref. 27.

[c] IACP scattering factors calculated from Eq. (3) using HF orbital energies for electron binding energies.

[d] IACP scattering factors calculated from Eq. (3) using experimental binding energies, Ref. 55.

al justification of this procedure Currat *et al.*[20] and Mendelsohn and Biggs[23] examined the scattering of a photon by an electron initially at rest in the laboratory frame to determine the appropriate multiplying factor for the Thomson cross section. Other authors[56,57] have referred to the Breit-Dirac correction factor, which goes as $(E_2^0/E_1)^3$. Both Mendelsohn and Biggs[23] and Currat[20] showed that in the nonrelativistic limit the Klein-Nishina formula[58] reduces to $(E_2^0/E_1)^2$ times the Thomson cross section. This argument is further supported by the behavior of the "exact hydrogenic" (EH) scattering factors calculated by Bloch and Mendelsohn.[24] The EH 1$S$, 2$S$, and averaged 2$P$ factors follow the $(E_2^0/E_1)^2$ curves for sufficiently large $E_1$ when plotted as a function of incident energy (cf. Fig. 14, Ref. 24).

An extensive comparison is shown between the IACP incoherent x-ray scattering factors calculated from Eq. (3) and the WH scattering factors determined by Brown[19] and Tavard.[18] Figure 1 and Tables I and II compare Brown's WH results with IACP factors computed for Mo $K\alpha$ and W $K\alpha$ radiation scattered by C. The angular dependence was taken over Brown's $s$ scale $[s = (\sin\theta)/\lambda]$. In Table III, Tavard's results are compared for Mo $K\alpha$ radiation scattered by B through Ne; however, in this case Tavard's "$q$ scale" $(q = 4\pi s)$ was used. All the IACP scattering factors shown in Tables I–III were calculated with both experimental electron binding energies (Exp. $E_B$), using Ref. 55 and HF orbital energies (HF $E_B$) as input parameters. This comparison was made to show the effect of different values of the electron binding energies upon the final scattering-factor results. Since the Exp. $E_B$ are slightly smaller than the HF $E_B$, the integration range over $q$ is extended, resulting in an over-all increase in the scattering factors calculated with Exp. $E_B$. This effect becomes negligible at large $s$, and these two sets of scattering factors converge. An attempt was made to modify the 1$S$ contribution by including 1$S$ binding energies computed for carbon in methane[59,60] along with an experimental 1$S$ value measured by Siegbhan[61,62] in connection with the 2$S$ and 2$P$ (Exp. $E_B$) parameters. This procedure reduced the Exp. $E_B$ scattering factors at large $s$, and the results from one of these calculations is reported in the fifth column of Table I. Table IV exhibits IACP scattering factors calculated for Mo $K\alpha$ and W $K\alpha$ radiation scattered by Li through Ne and using only the Exp. $E_B$ parameters. Results for carbon are omitted since they are extensively covered in Tables I and II. All inelastic scattering factors calculated in this research or discussed in this section are reported in electron units.

In the case of carbon the IACP scattering factors are substantially lower for $s < 0.6$ than the WH results obtained from HF wave functions by either Brown or Tavard. Tavard's results for carbon were compared graphically with Brown's HF values and found to be in very close agreement. In the region between $s = 0.3$ and 0.08 the IACP factors calculated using Exp. $E_B$ are within (1–3)% of the WH values computed by Brown using the 40-term CI wave function. Brown's HF values differ from his CI results in this $s$ region by at least 5% and this variation increases to 16% at $s = 0.1$ (see Table I, comparison of columns 2, 3, and 5). The curve representing the IACP (Exp. $E_B$) factors crosses Brown's curve for the CI results at $s = 0.28$ and 0.14, as shown in Fig. 1 and by the values given in Table I. No *a priori* reason exists for agreement that is even this close between the IACP factors and those obtained from a CI wave function in the above $s$ region. However, at small scattering angles, the IACP values should be substantially lower than the WH values when both are calculated from the same wave function. This effect is demonstrated in the comparison between

TABLE IV. IACP scattering factors for Mo $K\alpha$ and W $K\alpha$ scattered by Li through Ne. [a]

| $\frac{\sin\theta}{\lambda}$ (Å$^{-1}$) | $S$(Mo $K\alpha$) | $S$(W $K\alpha$) | $S$(Mo $K\alpha$) | $S$(W $K\alpha$) | $S$(Mo $K\alpha$) | $S$(W $K\alpha$) | $S$(Mo $K\alpha$) | $S$(W $K\alpha$) |
|---|---|---|---|---|---|---|---|---|
| | Li | | Be | | B | | N | |
| 0.025 | 0.010 26 | 0.010 26 | 0.017 86 | 0.017 89 | 0.029 38 | 0.029 42 | 0.039 31 | 0.039 41 |
| 0.050 | 0.040 29 | 0.040 37 | 0.045 21 | 0.045 29 | 0.163 26 | 0.163 50 | 0.284 74 | 0.285 38 |
| 0.075 | 0.260 51 | 0.260 95 | 0.179 71 | 0.180 13 | 0.406 37 | 0.407 07 | 0.688 85 | 0.690 41 |
| 0.100 | 0.626 87 | 0.627 94 | 0.557 93 | 0.559 12 | 0.780 82 | 0.782 38 | 1.164 25 | 1.167 19 |
| 0.125 | 0.926 76 | 0.928 70 | 1.042 86 | 1.045 13 | 1.234 99 | 1.237 77 | 1.654 07 | 1.658 71 |
| 0.150 | 1.131 42 | 1.134 47 | 1.461 47 | 1.465 08 | 1.682 38 | 1.686 69 | 2.125 74 | 2.132 41 |
| 0.175 | 1.286 58 | 1.290 98 | 1.762 60 | 1.767 83 | 2.065 75 | 2.071 91 | 2.560 93 | 2.570 01 |
| 0.200 | 1.424 10 | 1.430 04 | 1.969 94 | 1.977 11 | 2.369 34 | 2.377 72 | 2.950 12 | 2.962 01 |
| 0.225 | 1.555 75 | 1.563 40 | 2.120 23 | 2.129 64 | 2.602 57 | 2.613 54 | 3.290 03 | 3.305 15 |
| 0.250 | 1.683 38 | 1.692 90 | 2.240 31 | 2.252 24 | 2.782 42 | 2.796 36 | 3.582 35 | 3.601 16 |
| 0.275 | 1.805 60 | 1.817 14 | 2.345 57 | 2.360 27 | 2.924 99 | 2.942 28 | 3.831 30 | 3.854 31 |
| 0.300 | 1.920 61 | 1.934 30 | 2.443 56 | 2.461 27 | 3.043 10 | 3.064 10 | 4.042 69 | 4.070 38 |
| 0.350 | 2.124 15 | 2.142 58 | 2.628 00 | 2.652 37 | 3.237 20 | 3.266 57 | 4.376 32 | 4.414 92 |
| 0.400 | 2.290 14 | 2.313 92 | 2.798 74 | 2.830 55 | 3.402 18 | 3.441 10 | 4.625 08 | 4.676 54 |
| 0.450 | 2.421 11 | 2.450 85 | 2.952 54 | 2.992 56 | 3.550 94 | 3.600 46 | 4.819 15 | 4.885 30 |
| 0.500 | 2.522 05 | 2.558 40 | 3.086 81 | 3.135 83 | 3.686 53 | 3.747 62 | 4.977 79 | 5.060 33 |
| 0.550 | 2.598 37 | 2.641 97 | 3.200 92 | 3.259 71 | 3.808 93 | 3.882 55 | 5.112 49 | 5.212 98 |
| 0.600 | 2.654 95 | 2.706 44 | 3.295 68 | 3.365 04 | 3.917 56 | 4.004 64 | 5.229 76 | 5.349 65 |
| 0.650 | 2.695 89 | 2.755 90 | 3.372 71 | 3.453 42 | 4.012 17 | 4.113 64 | 5.333 19 | 5.473 85 |
| 0.700 | 2.724 48 | 2.793 63 | 3.433 97 | 3.526 83 | 4.093 00 | 4.209 77 | 5.424 70 | 5.587 42 |
| 0.750 | 2.743 32 | 2.822 20 | 3.481 49 | 3.587 27 | 4.160 65 | 4.293 65 | 5.505 35 | 5.691 38 |
| 0.800 | 2.754 42 | 2.843 62 | 3.517 16 | 3.636 62 | 4.216 02 | 4.366 14 | 5.575 76 | 5.786 27 |
| 0.900 | 2.759 27 | 2.870 76 | 3.559 56 | 3.708 58 | 4.293 97 | 4.480 98 | 5.687 45 | 5.950 36 |
| 1.000 | 2.747 68 | 2.883 54 | 3.572 30 | 3.753 62 | 4.335 07 | 4.562 32 | 5.762 90 | 6.082 49 |
| 1.100 | 2.724 89 | 2.886 99 | 3.563 42 | 3.779 57 | 4.346 82 | 4.617 42 | 5.805 55 | 6.185 88 |
| 1.200 | 2.694 11 | 2.884 13 | 3.538 62 | 3.791 86 | 4.335 45 | 4.652 21 | 5.819 24 | 6.264 01 |
| 1.300 | 2.657 39 | 2.876 83 | 3.501 90 | 3.794 24 | 4.305 90 | 4.671 33 | 5.807 79 | 6.320 35 |
| 1.400 | 2.616 10 | 2.866 24 | 3.456 10 | 3.789 26 | 4.262 04 | 4.678 31 | 5.774 80 | 6.358 11 |
| 1.500 | | 2.853 12 | | 3.778 70 | | 4.675 80 | | 6.380 11 |
| 1.600 | | 2.837 97 | | 3.763 79 | | 4.665 79 | | 6.388 80 |
| 1.800 | | 2.802 84 | | 3.724 18 | | 4.628 82 | | 6.374 21 |
| 2.000 | | 2.762 57 | | 3.674 89 | | 4.575 42 | | 6.327 06 |
| 2.200 | | 2.718 14 | | 3.618 42 | | 4.510 27 | | 6.256 07 |
| 2.400 | | 2.670 18 | | 3.556 28 | | 4.436 27 | | 6.167 21 |
| 2.600 | | 2.619 19 | | 3.489 50 | | 4.355 31 | | 6.064 67 |
| 2.800 | | 2.565 58 | | 3.418 83 | | 4.268 75 | | 5.951 44 |
| 3.000 | | 2.509 70 | | 3.344 91 | | 4.177 60 | | 5.829 75 |
| 3.200 | | 2.451 90 | | 3.268 25 | | 4.082 70 | | 5.701 33 |
| 3.400 | | 2.392 50 | | 3.189 35 | | 3.984 74 | | 5.567 57 |
| 3.600 | | 2.331 79 | | 3.108 63 | | 3.884 36 | | 5.429 62 |
| 3.800 | | 2.270 08 | | 3.026 52 | | 3.782 11 | | 5.288 47 |
| 4.000 | | 2.207 64 | | 2.943 39 | | 3.678 50 | | 5.144 98 |
| | O | | F | | Ne | | | |
| 0.025 | 0.079 07 | 0.079 26 | 0.064 53 | 0.064 73 | 0.053 21 | 0.053 41 | | |
| 0.050 | 0.525 80 | 0.526 87 | 0.503 89 | 0.505 20 | 0.477 63 | 0.479 17 | | |
| 0.075 | 1.058 17 | 1.060 43 | 1.088 95 | 1.091 80 | 1.100 08 | 1.103 57 | | |
| 0.100 | 1.539 25 | 1.543 04 | 1.627 27 | 1.631 96 | 1.696 21 | 1.701 93 | | |
| 0.125 | 1.987 86 | 1.993 60 | 2.106 27 | 2.113 23 | 2.219 56 | 2.227 91 | | |
| 0.150 | 2.424 34 | 2.432 46 | 2.552 17 | 2.561 87 | 2.688 49 | 2.699 96 | | |
| 0.175 | 2.847 85 | 2.858 78 | 2.980 74 | 2.993 66 | 3.126 18 | 3.141 31 | | |
| 0.200 | 3.248 33 | 3.262 47 | 3.393 80 | 3.410 41 | 3.545 19 | 3.564 49 | | |
| 0.225 | 3.616 21 | 3.634 02 | 3.786 09 | 3.806 86 | 3.948 09 | 3.972 08 | | |
| 0.250 | 3.946 30 | 3.968 22 | 4.151 26 | 4.176 66 | 4.331 99 | 4.361 19 | | |
| 0.275 | 4.237 26 | 4.263 81 | 4.484 93 | 4.515 47 | 4.692 55 | 4.727 47 | | |
| 0.300 | 4.490 96 | 4.522 67 | 4.785 12 | 4.821 33 | 5.026 30 | 5.067 48 | | |
| 0.350 | 4.900 93 | 4.944 59 | 5.288 45 | 5.337 70 | 5.607 10 | 5.662 54 | | |

TABLE IV *(Continued)*

| $\frac{\sin\theta}{\lambda}$ (Å$^{-1}$) | $S$(Mo $K\alpha$) | $S$(W $K\alpha$) | $S$(Mo $K\alpha$) | $S$(W $K\alpha$) | $S$(Mo $K\alpha$) | $S$(W $K\alpha$) | $S$(Mo $K\alpha$) | $S$(W $K\alpha$) |
|---|---|---|---|---|---|---|---|---|
| 0.400 | 5.208 91 | 5.266 74 | 5.678 84 | 5.743 52 | 6.076 00 | 6.148 15 | | |
| 0.450 | 5.444 70 | 5.518 88 | 5.980 83 | 6.063 34 | 6.448 29 | 6.539 71 | | |
| 0.500 | 5.630 69 | 5.723 27 | 6.216 83 | 6.319 54 | 6.742 85 | 6.856 13 | | |
| 0.550 | 5.782 19 | 5.895 10 | 6.404 49 | 6.529 66 | 6.977 05 | 7.114 73 | | |
| 0.600 | 5.909 15 | 6.044 19 | 6.556 72 | 6.706 49 | 7.165 00 | 7.329 54 | | |
| 0.650 | 6.017 86 | 6.176 70 | 6.682 54 | 6.858 91 | 7.317 54 | 7.511 24 | | |
| 0.700 | 6.112 18 | 6.296 38 | 6.788 15 | 6.993 01 | 7.442 66 | 7.667 74 | | |
| 0.750 | 6.194 48 | 6.405 53 | 6.877 76 | 7.112 87 | 7.546 22 | 7.804 74 | | |
| 0.800 | 6.266 20 | 6.505 50 | 6.954 18 | 7.221 19 | 7.632 38 | 7.926 27 | | |
| 0.900 | 6.381 27 | 6.681 00 | 7.074 36 | 7.409 77 | 7.763 63 | 8.133 63 | | |
| 1.000 | 6.461 70 | 6.826 73 | 7.157 71 | 7.567 11 | 7.851 66 | 8.304 20 | | |
| 1.100 | 6.510 37 | 6.945 18 | 7.208 93 | 7.697 33 | 7.904 58 | 8.445 35 | | |
| 1.200 | 6.530 06 | 7.038 73 | 7.231 08 | 7.802 98 | 7.927 14 | 8.561 16 | | |
| 1.300 | 6.523 72 | 7.109 94 | 7.226 82 | 7.886 22 | 7.922 59 | 8.654 24 | | |
| 1.400 | 6.494 35 | 7.161 37 | 7.198 72 | 7.949 15 | 7.893 56 | 8.726 65 | | |
| 1.500 | | 7.195 46 | | 7.993 83 | | 8.780 23 | | |
| 1.600 | | 7.214 43 | | 8.022 21 | | 8.816 75 | | |
| 1.800 | | 7.214 76 | | 8.037 25 | | 8.845 10 | | |
| 2.000 | | 7.175 44 | | 8.006 88 | | 8.823 57 | | |
| 2.200 | | 7.106 19 | | 7.941 13 | | 8.762 06 | | |
| 2.400 | | 7.014 07 | | 7.847 73 | | 8.668 58 | | |
| 2.600 | | 6.904 26 | | 7.732 60 | | 8.549 53 | | |
| 2.800 | | 6.780 60 | | 7.600 29 | | 8.410 00 | | |
| 3.000 | | 6.646 00 | | 7.454 34 | | 8.254 06 | | |
| 3.200 | | 6.502 72 | | 7.297 54 | | 8.084 98 | | |
| 3.400 | | 6.352 58 | | 7.132 15 | | 7.905 45 | | |
| 3.600 | | 6.197 07 | | 6.960 04 | | 7.717 69 | | |
| 3.800 | | 6.037 46 | | 6.782 75 | | 7.523 56 | | |
| 4.000 | | 5.874 83 | | 6.601 64 | | 7.324 68 | | |

[a] These IACP scattering factors were calculated from Eq. (3) using experimental binding energies, Ref. 55. $E_1$(Mo $K\alpha$) = 17.441 keV and $E_1$(W $K\alpha$) = 58.856 keV.

the IACP results for carbon and the HF carbon results computed by Brown and Tavard for $s < 0.6$. Detailed descriptions of this effect are given in the literature.[20,23,24] As the scattering angle is decreased, the $q$ cutoff limits [$q^m$, Eq. (24)] go to increasing $+q$ values. Under these conditions the integration region contains less than half of the profile and the largest possible value of $E_2$ for Compton scattering is less than $E_2^0$. The WH factors defined in terms of $(E_2^0/E_1)^2$ give a large overestimate of the scattering for these cases.[23,24]

The IACP factors calculated in this research for Mo $K\alpha$ radiation scattered by Li agree with the IA total cross sections determined by Currat *et al.* (cf. Table I, Ref. 20). At low scattering angles these authors found a difference of a factor of 3 between the WH and IA results for Ge.[20] The integrated Compton profile results determined for Ge by Currat *et al.*[20] showed substantial differences from the WH factors starting at $s = 0.7$, and were a factor of 3.6 higher at $s = 0.1$. The same trend found by Currat[20] for Ge was found in this research for the IACP O, F, and Ne factors when compared with Tavard's WH values (Table III) in the region below $s = 0.3$. Currat[20] studied large-angle scattering in order to facilitate the absolute normalization of experimental profiles. At higher scattering angles IACP's and the WH theory converge. An absolute measurement of the total inelastic scattered intensity for Mo $K\alpha$ radiation scattered from polycrystalline Be at $2\theta = 120°$ was performed by Phillips.[38] This intensity was found to be 3.556 after applying the $(E_2^0/E_1)^2$ correction factor. The IACP value for Mo $K\alpha$ radiation scattered by Be at 120° is 3.533, while the corrected WH value determined by Freeman is 3.537 (cf. Table II, Ref. 38). Freeman calculated inelastic scattering factors from the WH theory but used wave functions where correlation effects were included.[10-15]

At large scattering angles the contributions of the valence and outer electrons are only sizable in the region near the Compton-profile peak. Under these conditions the differences between WH and IACP total scattering cross sections are not very great. However, at low scattering angles the parameter $q^m$ becomes large for the core electrons,

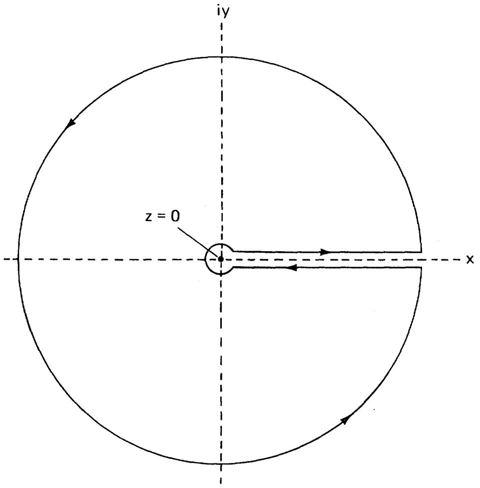

FIG. 2. Contour for evaluation of an integral with a branch point at $Z=0$.

reducing their integration range and contribution to the total inelastic scattering factor. The major contribution then comes from the valence and outer electrons whose binding energies are relatively small, and this condition enables the IA to accurately represent the electron-photon interaction. Even in cases where the shape of Compton profiles calculated from the IA did not agree with those computed from the exact theory, Bloch and Mendelsohn found sufficient "profile crossings" so that upon integration the resulting total cross sections matched closely. Compton profiles are easily calculated for complex atoms and molecules using the IA. The use of Compton profiles offers a realistic possibility for computing more accurate inelastic scattering factors than can be obtained from the Waller-Hartree theory.

## ACKNOWLEDGMENT

The author wishes to thank Dr. P. S. Ong for many helpful discussions during the course of this research.

## APPENDIX

A useful and straightforward method was developed for solving the cross-term integrals found in deriving closed-form expressions for $J(q)$. All of these integrals had the following functional form:

$$I=\int_{|q|}^{\infty}\frac{p^n\,dp}{(p^2+a^2)^m(p^2+b^2)^{\bar{m}}}, \tag{A1}$$

where $m$ and $\bar{m}$ are integers, $n$ is an odd integer, and both $a$ and $b$ are arbitrary constants. The integral in Eq. (A1) may be transformed by redefining the integration variables as

$$x^2=p^2-q^2, \tag{A2}$$

and by using

$$dp=x\,dx/(x^2+q^2)^{1/2}. \tag{A3}$$

Equation (A1) now becomes

$$I=\int_0^{\infty}\frac{(x^2+q^2)^{\bar{n}}x\,dx}{(x^2+c^2)^m(x^2+d^2)^{\bar{m}}}. \tag{A4}$$

The integration limits are extended from $x=0$ to $x=\infty$, $\bar{n}=\frac{1}{2}(n-1)$, and the quantities $c$ and $d$ are defined by $c^2=q^2+a^2$, $d^2=q^2+b^2$. The values of $n$, $m$, and $\bar{m}$ are such that the integrand goes to zero as $x\rightarrow$ zero and goes to zero faster than $x^{-2}$ as $x\rightarrow\infty$; additionally, there are no poles on the positive axis. These properties exhibited by the integrand in Eq. (A4) are identical to those required for type-3 integral described by Morse and Feshbach.[63] The example given in Morse and Feshbach[63] for a type-3 integral is valid only for noninteger values of $n$ or $\bar{n}$. In order to create a branch point at $Z=0$ for the case where $n$ is an integer, a $\ln(z)$ term is introduced in the integrand and a branch cut is taken along the positive real axis, as shown in Fig. 2. Using $zf(z)$ to represent the integrand in Eq. (A4), the integral around the contour in Fig. 2 is expressed as

$$\oint \ln z\, zf(z)\,dz\,. \tag{A5}$$

Since the integrals around the large and small circles vanish owing to the boundary conditions described above, the integration around the contour in Fig. 2 may be evaluated using the Cauchy theorem as

$$\begin{aligned}\oint \ln z\, zf(z)\,dz &= -2\pi i\int_0^{\infty} xf(x)\,dx+\int_0^{\infty}\ln x\, xf(x)\,dx\\ &\quad-\int_0^{\infty}\ln x\, xf(x)\,dx\\ &=2\pi i\times(\text{sum of the residues})\,.\end{aligned} \tag{A6}$$

Equation (A4) may now be solved by

$$\int_0^{\infty}\frac{(x^2+q^2)^{\bar{n}}x\,dx}{(x^2+c^2)^m(x^2+d^2)^{\bar{m}}}=-(\text{sum of the residues})\,. \tag{A7}$$

The residues are those of $\ln z\, zf(z)$ and are evaluated at all $n$th-order poles in the complex plane.

In order to check the results of Eq. (A7), another procedure was used in solving (A4). By a suitable transformation of the integration variable, Eq. (A4) may be evaluated in terms of the confluent hypergeometric function using formula 3.197-1 in Gradshteyn and Ryzhik.[64] A closed-form solution is then obtained using the integral representation for the hypergeometric function. Both of these methods produced identical results. The method based on the residue theorem was easier to use and is presented here because of its general usefulness in solving integrals where the integrand has the same functional form as the integrand in Eq. (A4).

---

*Research supported in part by Grant No. G-545 from the Robert A. Welch Foundation.

[1] I. Waller and D. R. Hartree, Proc. R. Soc. A 124, 119 (1929).

[2] G. Wentzel, Z. Phys. 43, 779 (1927).

[3] O. Klein, Z. Phys. 41, 407 (1927).

[4] A. H. Compton, Phys. Rev. 35, 925 (1930).

[5] C. V. Raman, Indian J. Phys. 3, 357 (1928).

[6] L. H. Thomas, Proc. Camb. Philos. Soc. 23, 542 (1927).

[7] E. Fermi, Z. Phys. 48, 73 (1928).

[8] W. Heisenberg, Phys. Z. 32, 737 (1931).

[9] L. Bewilogua, Phys. Z. 32, 740 (1931).

[10] A. J. Freeman, Phys. Rev. 113, 169 (1959).

[11] A. J. Freeman, Phys. Rev. 113, 176 (1959).

[12] A. J. Freeman, Acta Cryst. 12, 261 (1959).

[13] A. J. Freeman, Acta Cryst. 12, 274 (1959).

[14] A. J. Freeman, Acta Cryst. 12, 929 (1959).

[15] A. J. Freeman, Acta Cryst. 13, 190 (1959).

[16] D. T. Keating and G. H. Vineyard, Acta Cryst. 9, 895 (1956).

[17] R. F. Pohler and H. P. Hanson, J. Chem. Phys. 42, 2347 (1965).

[18] C. Tavard, D. Nicolas, and M. Rouault, J. Chim. Phys. 64, 540 (1967).

[19] R. T. Brown, Phys. Rev. A 5, 2141 (1972).

[20] R. Currat, P. D. DeCicco, and R. J. Weiss, Phys. Rev. B 4, 4256 (1971).

[21] R. J. Weiss, A. Harvey, and W. C. Phillips, Philos. Mag. 17, 241 (1968).

[22] R. A. Bonham, J. Chem. Phys. 43, 1460 (1965).

[23] L. B. Mendelsohn and F. Biggs, in *Proceedings of the International Conference on Inner Shell Ionization Phenomena and Future Applications, Atlanta, Georgia, 1972,* edited by R. W. Fink, S. T. Manson, J. M. Palms, and R. V. Rao, Conf-720 404 (Natl. Tech. Information Service, U. S. Dept. of Commerce, Springfield, Va., 1972), Vol. 3, pp. 1142–74.

[24] B. J. Bloch and L. B. Mendelsohn, Phys. Rev. A 9, 129 (1974).

[25] F. Bloch, Phys. Rev. 46, 674 (1934).

[26] P. Eisenberger and P. M. Platzman, Phys. Rev. A 2, 415 (1970).

[27] E. Clementi, IBM J. Res. Dev. Suppl. 9, 2 (1965).

[28] W. E. Duncanson and C. A. Coulson, Proc. Phys. Soc. Lond. 57, 190 (1945).

[29] J. B. Mann, J. Chem. Phys. 46, 1646 (1967).

[30] A. W. Weiss, Phys. Rev. 162, 71 (1967).

[31] L. B. Mendelsohn, F. Biggs, and J. B. Mann, Int. J. Quantum Chem. Symp. 7, 395 (1973).

[32] P. Eisenberger, Phys. Rev. A 5, 628 (1972).

[33] P. Eisenberger, J. Chem. Phys. 56, 1207 (1972).

[34] P. Eisenberger and W. A. Reed, Phys. Rev. B 9, 3237 (1974).

[35] P. Eisenberger, Phys. Rev. A 2, 1678 (1970).

[36] M. Cooper, J. A. Leake, and R. J. Weiss, Philos. Mag. 12, 797 (1965).

[37] M. Cooper and J. A. Leake, Philos. Mag. 15, 1201 (1967).

[38] W. C. Phillips and R. J. Weiss, Phys. Rev. 171, 790 (1968).

[39] R. J. Weiss and W. C. Phillips, Phys. Rev. 176, 900 (1968).

[40] W. C. Phillips and R. J. Weiss, Phys. Rev. 182, 923 (1969).

[41] W. A. Reed, P. Eisenberger, K. C. Pandey, and L. C. Snyder, Phys. Rev. B 10, 1507 (1974).

[42] P. Eisenberger and W. A. Reed, Phys. Rev. A 5, 2085 (1972).

[43] P. Eisenberger and W. A. Reed, Phys. Rev. B 9, 3242 (1974).

[44] R. Benesch and V. H. Smith, Jr., Phys. Rev. A 5, 114 (1972).

[45] R. E. Brown and V. H. Smith, Jr., Phys. Rev. A 5, 140 (1972).

[46] I. R. Epstein, Phys. Rev. A 8, 160 (1973).

[47] J. W. M. DuMond, Phys. Rev. 33, 643 (1929).

[48] J. W. M. DuMond, Phys. Rev. 36, 146 (1930).

[49] M. Cooper, Adv. Phys. 20, 453 (1971).

[50] A. H. Compton, Phys. Rev. 21, 483 (1928).

[51] J. B. Scarborough, *Numerical Mathematical Analysis* (Johns Hopkins U. P., Baltimore, Md., 1966), 6th ed.

[52] J. A. Bearden, Rev. Mod. Phys. 39, 78 (1967).

[53] E. W. White and G. G. Johnson, Jr., *X-ray and Absorption Wavelengths and Two-Theta Tables,* 2nd ed., ASTM Data Series DS37A (ASTM, Philadelphia, 1970).

[54] S. L. Adler, in *Atomic Physics III, Proceedings of the Third International Conference on Atomic Physics, Boulder, Colorado, 1972,* edited by S. J. Smith and G. K. Walters (Plenum, N. Y., 1973), p. 73.

[55] W. Lotz, J. Opt. Soc. Am. 58, 915 (1968).

[56] R. W. James, in *The Crystalline State,* Vol. II, edited by Sir Lawrence Bragg (G. Bell & Son, London, 1950).

[57] Y.-K. Kim and M. Inokuti, Phys. Rev. 165, 39 (1968).

[58] O. Klein and Y. Nishina, Z. Phys. 52, 853 (1929).

[59] F. A. Gianturco and M. Zandomeneghi, J. Chim. Phys. 71, 18 (1974).

[60] R. Moccia and M. Zandomeneghi, Chem. Phys. Lett. 11, 221 (1971).

[61] K. Siegbhan *et al., ESCA Applied to Free Molecules* (North-Holland, Amsterdam, 1969).

[62] K. Siegbhan, in Ref. 54, p. 493.

[63] P. M. Morse and H. Feshbach, *Methods of Theoretical Physics* (McGraw-Hill, N. Y., 1953), Part I, p. 410.

[64] I. S. Gradshteyn and I. M. Ryzhik, *Tables of Integrals, Series, and Products,* prepared by Yu. V. Geronimus and M. Yu. Tseytlin, (Academic, N. Y., 1965), 4th ed.